Report LR-743

The Synthesis of Flight Simulation Models: DATCOM Techniques versus Flight Test Identification

October 1993

M. Baarspul / J.A. Mulder

TU Delft

Faculty of Aerospace Engineering

Delft University of Technology

The Synthesis of Flight Simulation Models: DATCOM Techniques versus Flight Test Identification

M. Baarspul / J.A. Mulder

CONTENTS

	page
1. Introduction	5
2. DATCOM techniques	5
2.1 Digital DATCOM	5
2.2 The Smetana program	5
2.3 Re-scaling known models	6
3. DATCOM based airplane models	6
3.1 General	6
3.2 Aerodynamic model	6
3.3 Engine model	8
3.4 Flight control system model	8
3.5 Landing gear model	9
4. Airplane model identification	9
4.1 Flight test measurement system	9
4.2 Flight test program	10
4.3 System identification techniques	10
4.4 Flight test data analysis	11
4.5 Final Citation 500 models	12
4.5.1 Identification of ground effect	12
4.5.2 Development of the engine model	13
4.5.3 Identification of the flight control system model	13
4.5.4 Identification of the landing gear model	14

5. Comparison of DATCOM based and final model responses 14

5.1 General 14

5.2 DATCOM based versus final Citation 500 responses 14

5.3 POM comparisons 15

6. Concluding remarks 16

7. References 16

Tables 18

Figures 19

1. Introduction

The present trend in flight simulation for conversion and proficiency training is to exploit flight simulators in the operation of commuter and general aviation aircraft. Environmental restrictions as well as economic and flight safety considerations, and the appearance of 'low cost' flight simulators[1] have no doubt stimulated this trend. A problem is that adequate databases from which aerodynamic-, engine-, mass distribution-, flight control system-, and landing gear models can be composed are usually not available to the simulator manufacturer. It is possible then to embark on a flight test program for identification of these models. If the flight test program is carefully designed, this may be a good approach with the important additional advantage that during the flight test program a POM (Proof of Match) database may be generated which is crucial in FAA Level C/D simulator certification.[2]
A very cost effective alternative to flight testing is using DATCOM techniques for aerodynamic model building. The problem here is the verification, and the tendency of simulator acceptance pilots to enforce subjective changes of certain model parameters during evaluation.
The present paper compares the quality of models resulting from application of DATCOM techniques to models identified from flight test data. The comparison is made for the Cessna Citation 500, a light twin engined jet airplane, see Fig. 7.

2. DATCOM techniques

2.1 Digital DATCOM

In preliminary design studies a priori aerodynamic models are used which depend on neither windtunnel nor flighttest measurements. Currently, these models are used in 'low cost' flight simulators for commuter and general general aviation aircraft. One of the techniques to obtain these a priori models is the USAF Stability and Control Digital DATCOM.[3] The Digital DATCOM computer program calculates static and dynamic stability derivatives, high-lift and control device characteristics and the effects of the airplane engines. The calculations are based on the methods described in the USAF Stability and Control DATCOM,[4] using the airplane geometry and inertia characteristics as main inputs. The trim option of the program calculates aerodynamic data and control deflections for airplane trim at subsonic speeds. The Digital DATCOM addressable aiplane geometries include conventional (including canard), as well as unconventional (multi surface) configurations. Flight condition definition in Digital DATCOM requires airplane Mach number or velocity, and the atmospheric conditions as either altitude or freestream pressure and temperature, from which the Reynolds number is computed. For a detailed description of Digital DATCOM, reference is made to the User's Manual.[3] In the present work, the program proved to be a valuable tool in the generation of a priori aerodynamic and engine models.

2.2 The Smetana program

A second method to compose a priori aiplane models is the use of 'Computer Assisted Analysis of Aircaft Performance Stability and Control' by F.O. Smetana.[5] This book is written as a detailed user's manual accompanying a package of Fortran computer programs which compute most of the stability and control, and performance characteristics, based on airplane geometry, power plant, and inertial characteristics. However, the Smetana program is restricted to aircraft with moderate-to-high aspect ratio wings, operating at subsonic speeds. Therefore it is suitable in particular to compose general aviation a priori models. The program also includes subroutines which operate on input data specifying the control surface geometry, inertial characteristics, and gearing to compute the control forces and airplane

stability and control parameters like neutral points, maneuver points, stick force per g, static stick force stability, maximum attainable roll rate, etc.

2.3 Re-scaling known models

As a third 'method' in the composition of a priori airplane models, it may be possible to make use of available mathematical models and datapackages of similar aircraft. In particular the mass properties model, and the landing gear model,[6] for which often no data are available, may be subject to re-scaling.

3. DATCOM based airplane models

3.1 General

DATCOM based flight simulation models should preferably be formulated in accordance with the requirements prescribed by IATA.[7] The resulting models are rather comprehensive, and include different kinds of non-linearities. Coefficients or functions in these models which cannot be computed with e.g. DATCOM, are set to zero. Some of these coefficients or functions may be identifiable from flight tests later on. As an example, the DATCOM based models developed for the Cessna Citation 500 are briefly described below.

3.2 Aerodynamic model

The aerodynamic model consists of models of the three aerodynamic force coefficients and the three aerodynamic moment coefficients. The model for the aerodynamic lift coefficient, C_L, reads:

$$C_L = C_{L_{(BASIC)}} + C_{L_{(\delta_e)}} + C_{L_{(\delta_t)}} + C_{L_{(q)}} + C_{L_{(\dot{\alpha})}} + C_{L_{(n)}} + C_{L_{(SB)}} + C_{L_{(UC)}} + C_{L_{(GE)}} \quad (1)$$

where C_L denotes the total airplane lift coefficient and $C_{L_{(BASIC)}}$ is the basic airplane lift coefficient, which is developed further into:

$$C_{L_{(BASIC)}} = C_L(\alpha,M) + \Delta C_L(\alpha,\delta_f) + \Delta C_{L_\alpha}(M,h) \ .\alpha \quad (2)$$

Herein $C_L(\alpha,M)$ denotes the lift coefficient of the 'clean configuration' as a function of angle of attack (α) and Mach number (M). It is further expanded into:

$$C_L(\alpha,M) = C_{L_o}(M) + C_{L_\alpha}(M) \ .\alpha \quad (3)$$

where $C_{L_o}(M)$ is the lift coefficient at α equal to zero, as a function of M, see Fig. 1, and $C_{L_\alpha}(M)$ denotes C_{L_α} as a function of M (Fig. 2).

$\Delta C_L(\alpha,\delta_f)$ in (2) denotes the incremental lift as a function of α and wing flap angle (δ_f), see Fig. 3 and $\Delta C_{L_\alpha}(M,h)$ is the increment in C_{L_α} as a function of M and altitude h.

In (1) $C_{L_{(\delta_e)}}$ denotes the increment in lift coefficient due to elevator deflection (δ_e), which is developed further into:

$$C_{L_{(\delta_e)}} = [C_{L_{\delta_e}}(\alpha,M) + C_{L_{\delta_e}}(\alpha,\delta_f) + \Delta C_{L_{\delta_e}}(M,h) + \Delta C_{L_{\delta_e}}(\delta_e)] \cdot \delta_e \quad (4)$$

$C_{L_{\delta_e}}(\alpha,\delta_f)$ is shown in Fig. 4.

$C_{L_{(\delta_t)}}$ in (1) denotes the increment in lift coefficient, due to elevator trimtab deflection (δ_{t_e}) and is written as:

$$C_{L_{(\delta_t)}} = C_{L_{\delta_{t_e}}}(\alpha,M) \cdot \delta_{t_e} \quad (5)$$

$C_{L_{(q)}}$ in (1) denotes the increment in lift coefficient due to pitch rate q, and is written as:

$$C_{L_{(q)}} = K_{q_L}(x_{c.g.}) \cdot [C_{L_q}(M,h) + \Delta C_{L_q}(M,\delta_f)] \cdot \frac{q\bar{c}}{V} \quad (6)$$

In (6) $K_{q_L}(x_{c.g.})$ denotes the correction factor for the center of gravity (c.g.) location. A similar expression may be written for $C_{L_{(\dot{\alpha})}}$ in (1):

$$C_{L_{(\dot{\alpha})}} = K_{\dot{\alpha}_L}(x_{c.g.}) \cdot [C_{L_{\dot{\alpha}}}(M,h) + \Delta C_{L_{\dot{\alpha}}}(M,\delta_f)] \cdot \frac{\dot{\alpha}\bar{c}}{V} \quad (7)$$

The last four terms in (1) read respectively:

$$C_{L_{(n)}} = [C_{L_n}(M,h) + \Delta C_{L_n}(M,\delta_f)] \cdot (n-1) \quad (8)$$

where n is the normal load factor (g).

$$C_{L_{(SB)}} = K_{SB}(\delta_{SB}) \cdot [C_{L_{SB}}(\alpha,M) + \Delta C_{L_{SB}}(\alpha,\delta_f)] \quad (9)$$

where $K_{SB}(\delta_{SB})$ denotes the speedbrake (SB) effectiveness factor as a function of speedbrake deflection angle (δ_{SB}); $C_{L_{SB}}(\alpha,M)$ and $\Delta C_{L_{SB}}(\alpha,\delta_f)$ are increments in lift coefficient due to full speedbrake deflection as functions of α, M and δ_f respectively.

$$C_{L_{(UC)}} = K_{UC}(\tau_{LG}) \cdot [C_{L_{UC}}(\alpha,\delta_f) + \Delta C_{L_{UC_M}}(\alpha) \cdot M] \quad (10)$$

where $K_{UC}(\tau_{LG})$ denotes the influence factor for a given degree of undercarriage (UC) extension (τ_{LG}).

$C_{L_{UC}}(\alpha,\delta_f)$ is the change in lift coefficient due to full landing gear extension as a function of α and δ_f; $\Delta C_{L_{UC_M}}(\alpha)$ denotes $\frac{\partial C_{L_{UC}}}{\partial M}$ as a function of α.

$$C_{L_{(GE)}} = K_{GE_L}(h_R) \cdot [C_{L_{(BASIC)_{GE}}}(\alpha,\delta_f) + C_{L_{\dot{\alpha}_{GE}}}(\delta_f).\frac{\dot{\alpha}\bar{c}}{V} + C_{L_{\delta_{e_{GE}}}}(\alpha,\delta_f) \cdot \delta_e] \quad (11)$$

where $K_{GE_L}(h_R)$ denotes the groundeffect (GE) influence factor on the lift coefficient as a function of radio altitude (h_R), see Fig. 5.

$C_{L_{(BASIC)_{GE}}}(\alpha,\delta_f)$ is the increment in basic lift coefficient due to ground effect at zero radio altitude as a function of α and δ_f;

$C_{L_{\dot{\alpha}_{GE}}}(\delta_f)$ is the increment in $C_{L_{\dot{\alpha}}}$ due to groundeffect at zero radio altitude as a function of δ_f; $C_{L_{\delta_{e_{GE}}}}(\alpha,\delta_f)$ is the increment in $C_{L_{\delta_e}}$ due to groundeffect at zero radio altitude as a function of α and δ_f.

In Ref. 7 similar expressions are given for the aerodynamic drag coefficient (C_D), the sideforce coefficient (C_Y), the pitching moment coefficient (C_m), the rolling moment coefficient (C_ℓ) and the yawing moment coefficient (C_n).

In Section 4.5 the DATCOM based aerodynamic lift coefficient will be compared to the lift coefficient in the final aerodynamic model, resulting from flight test data analysis.

3.3 Engine model

For the a priori engine model, data was obtained from the General Installed Turbofan Performance Computer Program (P1532C) issued by United Aircraft of Canada Ltd. for the commercial version of the Pratt & Whitney (Canada) JT15D turbofan engine. The program, which is of the curve reading type, may be used to generate power setting values of fan speed, resulting in not less than minimum rated thrust on production engines. An example of the calculations performed using this program is presented in Fig. 6, where pressure corrected net thrust XN/δ_1 is plotted versus temperature corrected fan speed $N_1/\sqrt{\theta_2}$ as a function of M and flight level (FL).

The major further development of the engine model was the transient model for realistic variations of all engine parameters with Power Lever Angle (PLA) command, including start-up and shut-down, see Section 4.5.

3.4 Flight control system model

The flight control system of the Citation 500 is fully mechanical. Aerodynamic hinge moments, mechanical inertia, friction and flexibility must therefore be included in a model of this flight control system. A second order system model was used for the primary flight control dynamics. The equation of motion, used for the computation of the control column-, control wheel- and rudder pedal deflections (s) reads:[8]

$$F = m\ddot{s} + W\dot{s} + Cs + F_{AER} + F_{COUL} + F_{STOP} + F_G + F_{NOSE}$$

where F denotes the control force applied by the pilot, m is the reduced mass of the flight controls, W denotes the viscous friction and C the spring stiffness. F_{AER}, F_{COUL}, F_{STOP} denote the aerodynamic, coulomb and mechanical stop force respectively, F_G denotes the force due to static unbalance and F_{NOSE} is the nose-wheel steering force on the rudder pedals, the Citation nose wheel steering being connected to these pedals via springs.

In Section 4.5, the final flight control system model will be described which resulted from the identification of the Citation 500 flight controls, using flight test measurements.

3.5 Landing gear model

In the a priori landing gear model, describing the conventional tri-cycle landing gear of the Citation, three submodels are being considered, i.e. those for the vertical forces, the side forces and the longitudinal forces respectively.[9] These are the forces acting on the aircraft due to ground contact. For the simulation of 'minimum unstick speed' a tailscraper was added to the model.
In Section 4.5, the final landing gear model, resulting from flight and taxi tests, will be briefly described.

It is possible to implement the DATCOM based aiplane models in a flight simulator host computer for evaluation with the pilot-in-the-loop. This gives the opportunity to check the general characteristics of these models at an early stage in the model development process.

4. Airplane model identification

4.1 Flight test measurement system

Airplane model identification includes the selection of an airborne measurement system and the specification of the aircraft configuration, flight conditions and maneuvers for system identification.[10] The measurement system is primarily required to measure the time-histories of input and output variables. In the high accuracy flight test measurement system, which was designed and build by the National Aerospace Laboratory (NLR),[11] four more-or-less independent sensor systems can be distinguished, see Fig. 7:
- Inertial measurement system
- Air-data measurement system, and α- and β vanes
- Transducers to measure engine parameters
- Transducers to measure control forces and displacements, control surface and trim deflections, landing gear parameters like shock absorber deflections, and nosewheel steering angle.

A Honeywell laser-gyro Inertial Reference System (IRS) measures specific aerodynamic or ground reaction forces and aircraft body rotation rates and accelerations. High accuracy pressure transducers in a temperature controlled box were used to measure airspeed and altitude variations in quasi steady flight. A variety of other variables was measured in addition, such as primary control forces and displacements, elevator, aileron, rudder and trimtab deflections, angle of attack and side-slip angle, using a specially designed nose boom. Where possible, standard onboard systems were used, such as for the measurement of engine speeds, inter-turbine temperature (ITT) and fuel flow, fuel quantity, stick shaker, anti skid warning, landing gear down- and up-locks, speed brakes extended/retracted and radar altitude. All these physical quantities were converted into electrical signals, which after signal conditioning are digitized using a Remote Multiplexer Digitizer Unit. Data from modern avionics that complied with the ARINC standard were processed using an ARINC multiplexer. Digitized data were stored on a 14 track magnetic tape recorder with enough capacity to allow continuous recording of all transducer outputs during the complete test flight, from before engine start until after engine shut down. A reference time signal was recorded on a separate track for correlation of the data tracks. Transducer signals were, depending on frequency contents, sampled with sample frequencies ranging from 2 to 50 Hz. However, for vibration measurements, three accelerometers positioned in the cockpit were sampled at a frequency of 256 Hz. Also sound measurements were recorded in another Citation cockpit, using two microphones.[12]

The first stage of post flight data processing consisted of adding the time to the measured data, using a frame synchronizer and expressing the recorded data in engineering units. The recorded data were corrected according to the calibration information of the measured channel and properly grouped to be used in the second stage of data analysis concerned with aircraft state reconstruction and mathematical model identification, see Section 4.3.

4.2 Flight test program

The flight test program, carried out with the instrumented Citation, was designed such that flight test maneuvers were evenly distributed in the admissible flight envelope. Two types of flight test maneuvers were applied for model identification:

- quasi-stationary maneuvers for large but slow variations of input and state variables;
- dynamic maneuvers for fast but small variations of input and state variables.

The quasi-stationary maneuvers were performed to evaluate nonlinear effects in the aerodynamic and flight control system models. Examples of quasi-stationary maneuvers were accelerations and decelerations at constant thrust and altitude, 'slow' pull-up-push-down maneuvers, side slips with varying side-slip angles, trimtab excursions at a constant nominal flight condition and wind-up turns.

The dynamic maneuvers were carried out to determine the dynamic stability and control characteristics of the aircraft. Examples of dynamic maneuvers were the responses to manually implemented, approximately block-shaped control displacements. These so-called doublets were sequentially implemented on the elevator, ailerons, rudder and left and right power levers, starting from steady, straight flight.

Quasi-stationary and dynamic maneuvers were executed for all relevant and admissable flight conditions and aircraft configuration combinations. In addition, extensive measurements were taken of dynamic engine reponses, airplane stalls, aerodynamic ground effects, take off and landing performance and ground handling characteristics.

4.3 System identification techniques

In order to identify the airplane models, described in Section 2, two different types of system identification techniques[13] were applied. The first type (type 1) of system identification technique may be characterized as 'model-adjustment technique', see Fig. 8. The idea is to implement a simulation model in the computer and to drive the model with the same inputs as the actual system. If the simulated output differs from the output of the actual system, curve 1 in Fig. 8, this must be caused by a difference in initial conditions and/or the parameters in the simulation model, having wrong values. Next, some usually quadratic-function of the difference between actual and simulated output is minimized with respect to both initial conditions and model parameter values. The technique may be interpreted in terms of statistical estimation theory. The optimal parameter values produce the minimum value of the so-called Likelihood Function and may result in the simulation curve 2 in Fig. 8.

The second type (type 2) of system identification technique is based on explicit mathematical relations, expressing parameter values in terms of system input and output measurements. The so-called 'equation error' methods fall in this category. The explicit mathematical relations follow immediately from regression analysis. In cases where the model structure is not yet precisely known, type 2 identification technique results in a much easier model developments process than type 1 identification technique.

In the present series of flight test measurements, the presence of virtually perfect accelerometers and rate gyro's in the measurement system was fully exploited. The corresponding signals i.e. specific external forces and body rotation rates were interpreted as input signals to a dynamic system model describing the evolution of the aircraft's state.[14] A state reconstruction

problem was defined, which was readily solved by applying a type 1 system identification technique. Computed time histories, of for instance airspeed and side slip angle, were matched to corresponding measured time histories by selecting 'optimal' initial conditions and estimating (very small) transducer bias errors. This resulted in an accurate and complete state vector trajectory estimate. As the model was virtually exactly known, the state reconstruction problem needed to be solved only once for each particular flight test maneuver. The main advantage of carrying out a state reconstruction is, that next a type 2 system identification technique may be applied to estimate the aerodynamic derivatives, see Table 1. Herein the simulation models are shown below the system identification technique applied. The performance of this 'two step' method to identify the aerodynamic derivatives is demonstrated in the 'Proof of Match' time histories in Section 5.

4.4 Flight test data analysis

The analysis and modelling of the aerodynamic lift coefficient (C_L) is now described as an example, using the above two-step identification technique. At the start of the analysis it was decided to concentrate in the first instance on the quasi-stationary-horizontal symmetrical reference conditions and the corresponding dynamic maneuvers at the test conditions in the entire flight envelope. The analysis of these test conditions was used both for the evaluation of the performance model as well as for the additional stability and control parts. Fig. 9 presents the test points for the clean configuration in a C_L-Mach plot. As a reference, also plotted herein are M^2C_L over corrected aircraft weight curves at four test altitudes. The aircraft weight (W) is chosen to represent the mean value of the test weights at that particular altitude. Additionally, in Fig. 9 the C_L excursions as a result of elevator doublets with large amplitude are depicted. The figure also shows the low speed stall and the high speed buffet boundaries for the clean configuration. For each test point in the flight envelope, a submodel was postulated for the three aerodynamic force (C_D, C_L, C_Y) and moment coefficients (C_m, C_ℓ, C_n) in the model axes reference frame, F_{mo}.

The submodel for the lift coefficient, expressed in equation (12), is valid within the normal flight envelope, which means that stall phenomena, buffeting, ground effect, etc. are not represented:

$$C_L = C_{L_0} + C_{L_\alpha} . \alpha + C_{L_{\alpha^2}} . \alpha^2 + C_{L_q} . \frac{q\bar{c}}{V} + C_{L_{\delta_e}} . \delta_e \qquad (12)$$

Because of the size of the aircraft and the speed regime of interest, the aircraft was assumed to be rigid. This eliminated the need for dynamic modelling of additional degrees of freedom due to flexibility.

Fig. 10 shows test points at constant altitude and c.g. position in a C_L-α plot. Because different Mach numbers are attached to each C_L value, Mach effects are embedded. Apart from the reference conditions, the α-sweeps are shown as a result of the elevator doublets. Because the α-sweeps were performed at approximately constant Mach number, Fig. 10 shows that C_L is described by different curves for each aircraft configuration and Mach number. After integration of the submodels for the lift, drag and pitching moment, it was possible for example to construct C_L/C_D curves for various Mach numbers. Fig. 11 shows these curves for the clean configuration resulting from the analysis. Also presented in this figure are the test points at the four flight test altitudes. For all configurations of interest, the coefficients in the submodels were determined using regression analysis and subsequently integrated to $C_L(M)$-α, $C_D(M)$-α and $C_m(M)$-α plots for increasing Mach numbers.

The clean configuration was considered as a base. Effects due to flap, gear and speedbrake extension were modelled as incremental contributions, which were superimposed on the base model.
As a result of the data processing, a large data set of stability and control derivatives was obtained, valid for the individual test conditions. In accordance with the model for the lift coefficient, these coefficients were formulated as global functions of angle of attack.

4.5 Final Citation 500 models

As a result of the flight test data analysis, the final aerodynamic lift coefficient shows the following modifications, when compared to the DATCOM based lift coefficient, described in Section 3:
In equation (1) the terms $C_{L_{(\delta_t)}}$, see equation (5), and $C_{L_{(n)}}$, see equation (8), could not be identified, so they were deleted. The lift coefficient for the clean configuration as a function of α and M, $C_L(\alpha,M)$, equation (3), is shown in Fig. 12, replacing the Figs. 1 and 2. Fig. 3, presenting $\Delta C_L(\alpha,\delta_f)$, see equation (2), was replaced by Fig. 13. In equation (4) the terms $\Delta C_{L_{\delta_e}}(M,h)$ and $\Delta C_{L_{\delta_e}}(\delta_e)$ could not be identified, so they were dropped. Fig. 14 shows $C_{L_{\delta_e}}(\alpha,\delta_f)$ in this equation. In equation (6), $C_{L_q}(M,h)$ was replaced by $C_{L_q}(\alpha,\delta_f)$, see Fig. 15. The term $\Delta C_{L_q}(M,\delta_f)$ was deleted from this equation, as it could not be identified. For operation in the normal flight envelope, the contribution of $C_{L_{(\dot\alpha)}}$, equation (7), was embedded in the contribution of $C_{L_{(q)}}$, as was already mentioned in Section 3.2. In equation (9) the term $\Delta C_{L_{SB}}(\alpha,\delta_f)$ could not be identified, so it was eliminated. In equation (10) the term $\Delta C_{L_{UC_M}}(\alpha) \cdot M$ was deleted, but a new term $C_{L_{q_{UC}}}(\alpha,\delta_f) \cdot \frac{q\bar{c}}{V}$ was added.

4.5.1 Identification of ground effect

In order to identify the contribution of ground effect to the lift, drag, pitching moment and rolling moment of the Citation 500 the 'two step' method as described in Subsection 4.3 was applied, using the "Interactive Flight Test Data Analysis Program Package".[17] The results of one of the identification methods used, the so called Combined Gauss-Newton/Linear Regression (CGNLR) method[18], are presented here. In order to perform the identification of $C_{L_{(GE)}}$ the a priori model (eq. 11) was modified as follows:

$$C_{L_{(GE)}} = k_{L_{0h}} \cdot C_{L_{0h}} \cdot h^{s_{L0}} + k_{L_{\alpha h}} \cdot C_{L_{\alpha h}} \cdot h^{s_{L\alpha}} + k_{L_{qh}} \cdot C_{L_{qh}} \cdot h^{s_{Lq}} + \\ + k_{L_{\delta_e h}} \cdot C_{L_{\delta_e h}} \cdot h^{s_{L\delta}} \qquad (13)$$

Similar modifications were made to the expressions for the drag and pitching moment coefficients due to ground effect. A new expression was added for the rolling moment coefficient due to ground effect:

$$C_{\ell_{(GE)}} = k_{(C_L\phi)} \cdot h^{s_{\ell\phi}} \qquad (14)$$

Table 2 presents the results of the identification of the parameters in the equations (13) and (14) for 40° flap deflection as far as height dependance could be identified. Fig. 16 shows the lift coefficient C_L as a function of α as a result of the CGNLR identification method for four different altitudes and 40° flap deflection. In Fig. 17 the rolling moment coefficient C_ℓ as a function of $C_L.\phi$ is presented for the same configuration, showing that ground effect tries to zero the roll angle ϕ.

Results of the identification of the complete aerodynamic model are presented in Section 5 in the form of 'Proof of Match' time histories.

4.5.2 Development of the engine model

The engine model for the P&W JT15D-1 engines was decomposed into two submodels:

- Static engine thrust model
- Dynamic engine model

For the final static engine performance model, the P1532C computer program was used, see Section 3.3, complemented with existing testbank data. From a comparison of partial climb recordings of the aircraft and the simulation model, it turned out, that for engine settings above 90% fan rpm (N1) the model showed superior climb performance relative to the aircraft. Because the angle of attack in flight and simulation corresponded very well in these cases, a discrepancy in the engine model was suspected at high power settings. From an analysis of both partial climb and aircraft longitudinal acceleration measurements, a correction was applied to the static thrust performance data at the higher power settings.
The dynamic engine model, which is very important in real-time simulation, was developed starting from a basic turbofan engine model. Flight test data during throttle chops and slams were available for the analyses of the engine dynamics. From these data the characteristic functions, parameters and time constants in the model were determined. Power change dynamics of the final engine model are demonstrated in the form of a 'Proof of Match' in Section 5.

4.5.3 Identification of the flight control system model

As the Citation 500 is equipped with a fully manual flight control system (FCS), the aerodynamic hinge moments on the control surfaces must be counter balanced by pilot generated control forces. Therefore a model of the aerodynamic hinge moments was an essential part of the FCS model and the identification[15] had to be based on measurements in flight. Model development started from a small set of flight test measurements in one flight condition and for one aircraft configuration. Fourth order models of the elevator and rudder FCS, where only the masses of the forward system (control column and rudder pedals respectively) and the aft system (elevator and rudder) were taken into account, were found to result in an adequate fit to the measured control and surface displacements. The aileron FCS required a 6th rather than a 4th order system model, to account for the masses of the control wheel and each of the ailerons. Since the FCS model represents a dynamical system, type 1 identification methods were applied for selection and estimation of the model parameters. In the analysis of the flight test maneuvers in all other flight conditions and aircraft configurations, the form of the FCS models was kept constant. This analysis resulted in a detailed map of aerodynamic hinge moment derivatives, which was subsequently implemented in the global FCS simulation model of the Citation.

4.5.4 Identification of the landing gear model

The final landing gear model of the Citation consists of four submodels, i.e. the wheel compression and gear strut model, the landing gear side force model, the main wheel brake model and the nose wheel steering model. Type 1 and type 2 identification techniques were used to identify these landing gear submodels, see Table 1. Due to the availability of the IRS, providing high accuracy time histories of the external specific forces on the aircraft, the body rotation rates, accelerations and attitude angles, type 2 identification technique could be applied to identify the wheel compression/gear strut and main wheel brake models. The landing gear side force model[9] could be identified using type 1 identification technique on a dynamical model, wherein the wheel slip angles were explicitly calculated. As mentioned already, the nose wheel steering system of the Citation is connected via springs to the rudder pedals. Type 1 identification technique was applied to identify second and fourth order dynamical nose wheel steering models. However, it turned out, that a quasi-static model performed surprisingly well. In the final landing gear simulation model, the tyre and strut deflections and rates of deflection are computed first, resulting in the vertical forces. These forces play a crucial role in the computation of the side forces and the longitudinal landing gear forces. Parameters related to the condition of the runway surface may have large effects on the magnitudes of these forces and consequently on the landing gear behaviour. As the ground measurements during taxi tests were performed on dry concrete, no effects of runway condition could be determined. Therefore, relevant data from available literature[9] was incorporated in the model. To prevent unrealistic behaviour of the simulated landing gear at zero aircraft speed, so called zero-speed models were added to the brake force, the side force and the nose wheel steering models.

5. Comparison of DATCOM based and final model responses

5.1 General

A quantitative validation of the quasi-stationary and dynamic characteristics of the DATCOM based as well as the final Citation models is possible, using the 'Proof of Match' (POM). In the POM simulated airplane responses are directly compared to aircraft flight traces providing for an objective examination of the mathematical model fidelity. For the generation of POM-data the data-files resulting from flight tests are read from the flight test tapes. In this manner the control forces and displacements, control surface position and power lever angles, as measured by the flight test measurement system, are used as the input signals to the six Degrees of Freedom (DOF) engineering simulation[6] of the Citation. The responses on these input signals are plotted against the same responses as measured in the aircraft during special flight test maneuvers.[16] The next Section describes some POMs of the DATCOM based and the final Citation 500 models.

5.2 DATCOM based versus final Citation 500 model responses

In order to compare the DATCOM based and final mathematical models and data of the Citation 500, POMs of both models were generated and subsequently plotted in one figure. By taking modelling data from the final into the DATCOM based models, the cause of the differences between the responses of both models was examined. For the DATCOM based models corrected in this manner, new POMs were generated in order to check if the correction made sense. Examples of the POMs of the DATCOM based, the corrected DATCOM based, and final Citation 500 models are presented below.

5.3 POM comparisons

POM comparisons are presented for the following models:
- the aerodynamic model
- the engine model
- the integrated Citation 500 simulation model

The POM comparisons of the aerodynamic models concern the airplane 'short period dynamics' with full flaps and gear down, and the 'roll response' in the clean configuration. Fig. 18 shows the pitch response (THETA) due to an elevator step-input and release after two seconds.
Comparing the pitch response of the DATCOM based model (dotted line) with the measured aircraft response shows a discrepancy which is out of FAA Level C tolerance. Taking the change in lift coefficient due to full landing gear extension $C_{L_{UC}}(\alpha, \delta_f)$, eq. (10), from the final aerodynamic model, results in an improved response of the 'corrected DATCOM based model' (dashed line). The final aerodynamic model response fits the measured response almost perfectly.

Fig. 19 shows the roll rate response (p) due to an aileron block-shaped input during five seconds.
Comparing the roll rate response of the DATCOM based model (dotted line) with the measured aircraft response shows a discrepancy which is just out of FAA Level C tolerance. Taking the increment in rolling moment coefficient due to roll rate ($C_{\ell_{(p)}}$) from the final aerodynamic model, results in a roll rate response of the 'corrected DATCOM based model' (dashed line) which is within FAA Level C tolerance. Also here the final aerodynamic model response fits the measured response almost perfectly.

The POM comparison of the engine model concerns the 'power change dynamics' of the P & W JT15D turbofan engine. Fig. 20 shows the change in Net Thrust (TN1) due to a power lever angle (PLA) change from 32° to idle in two seconds.
Comparing the response of the DATCOM based engine model (dotted line) with the measured engine response shows a significant difference in the starting value of the thrust at 32° PLA. The DATCOM based engine model dynamics are not correct either, however the thrust at idle power is correct. In the 'corrected DATCOM based model' (dashed line) the table of HP rotor speed has been adapted to the measured stationary starting value. Morover the engine model time-constant (τ) has been halved. The figure shows that the 'corrected DATCOM based model' response is now closer to the measured engine response than the 'final model' response (dot-dash line).

The POM comparison of the integrated Citation 500 model concerns the 'normal take-off'. Fig. 21 shows the aircraft pitch angle (THETA) and radio altitude (H-RADIO) during this maneuver.
Comparing the pitch response of the DATCOM based model (dotted line) with the measured aircraft pitch response shows a significantly smaller pitch angle of the DATCOM based model. The response of radio altitude shows that the DATCOM based Citation leaves the runway too late. Taking the values for the length of the nose gear, the change in lift coefficient due to ground effect, $C_{L_{(GE)}}$ (eq. 11), and the change in pitching moment coefficient $C_{m_{(GE)}}$ due to ground effect from the current Citation model, results in an almost perfect response of the 'corrected DATCOM based model' (dashed line). In this case the final model response, including the identification of ground effect as described in Section 4.5.1, has as yet to be made.

6. Concluding remarks

DATCOM techniques were compared to flight test identification in composing a flight simulation model. On the basis of this comparison, it has been shown that quite acceptable DATCOM based models can indeed be composed using inexpensive DATCOM techniques. Many model improvements were possible, however, by using the results of an extensive flighttest program. These model improvements were thought to warrant the extra costs of the flighttest program. Further more, since FAA Level C/D simulator approval requires a successful Proof of Match, flight testing is necessary anyway. The balanced use of both techniques in the synthesis of flight simulation models may lead to smaller flighttest programs and reduced costs of flight validated models. 'Low cost' flight simulators for commuter airlines and general aviation training may benefit from this development.
For the present, work is in progress to upgrade the Citation 500 mathematical models to represent the Citation II, the new laboratory jet aircraft jointly operated by the Dutch National Aerospace Laboratory (NLR), and the Faculty of Aerospace Engineering of Delft University of Technology.

7. References

1. Baarspul, M., Brönnimann, Ch., Conijn, C. (1991). A 'Low-Cost' Full Flight Simulator for Basic IFR Training. Royal Aeronautical Society conference on: Flight Simulation - European Opportunities, London UK.

2. Anon. (1991). Airplane Simulator Qualification. Advisory Circular AC 120-40B. U.S. Department of Transportation, Federal Aviation Administration.

3. Williams, J.E., Vulkelich, S.R. (1979). The USAF Stability and Control Digital Datcom, Vol. I, Users Manual, Technical Report AFFDL-TR-79-3032, Vol. I. McDonnell Douglas Astronautic Company, St.Louis Missouri 63166, USA.

4. McDonnell Douglas Corp. (1976). USAF Stability and Control Datcom. Air Force Flight Dyn. Lab., U.S. Air Force.

5. Smetana, F.O. (1984). Computer Assisted Analysis of Aircraft Performance Stability and Control. McGraw-Hill Book Company, ISBN 0-07-58441-9.

6. Baarspul, M. (1990). A review of flight simulation techniques. In: Progress in Aerospace Sciences, An International Review Journal Volume 27 Number 1, ISSN 0376-0421, Pergamon Press, Oxford, UK.

7. IATA (1986). Flight Simulator Design and Performance Data Requirements (Final draft of proposal revision A).

8. Baarspul, M., Dooren, J.P. van, (1976). The Hybrid Simulation of Aircraft Motions in a Piloted Moving-base Flight Simulator. Report VTH- 178, Delft University of Technology, Delft, The Netherlands.

9. Wahi, M.K., Yourkowski, F.M. (1980). 757-200 crew training simulator-ground handling data. Boeing Commercial Airplane Company, Seattle, USA.

10. Klein, V. (1989). Estimation of aircraft aerodynamic parameters from flight data. In: Progress in Aerospace Sciences, An International Review Journal Volume 26 Number 1, Pergamon Press, Oxford, UK.

11. Nieuwpoort, A.M.H., Breeman, J.H., Baarspul, M., Mulder, J.A. (1988). Phase II Flight Simulator Mathematical Model and Data-Package, Based on Flight Test and Simulation Techniques. In: ICAS Proceedings 1988, Vol. 2, Paper ICAS-88-1.9.2, 16th Congress of the International Council of the Aeronautical Sciences, Jerusalem, Israel.

12. Ruijgrok, G.J.J., Paassen, D.M. van, (1987). Sound Measurements of the Cessna Citation PH-CTE. Memorandum M-565, Delft University of Technology, Delft, The Netherlands.

13. Eijkhoff, P. (1974). System identification. John Wiley & Sons, ISBN 0-24980-7.

14. Mulder, J.A. (1987). Design and Evaluation of Dynamic Flight Test Manoeuvres. Report LR-497, Delft University of Technology, Delft, The Netherlands.

15. Mulder, J.A. (1988). Aircraft flight control system identification. In: Proceedings of 8th IFAC-IFORS Symposium on Identification and System Parameter Estimation. Beijing, China.

16. Anon. (1987). Citation 500 aircraft pilot test procedures for FAA Phase II ATG manoeuvres, Revision 1, CAE Electronics Ltd., Montreal, Canada.

17. Brug, G. van de, (1992). Implementation of aerodynamic model identification algorithms in the Interactive Flight Test Data Analysis Program Package. Thesis report, Delft University of Technology, Delft.

18. Leeuwen, H.J.van, (1992). Ground effect on the Cessna Citation (in Dutch). Thesis report, Delft University of Technology, Delft, The Netherlands.

System Identification Technique	
Type 1	**Type 2**
Aircraft state trajectory	Aerodynamic forces and moments
Dynamic engine response	Static engine performance
Flight control system	Flight control system
Landing gear side forces	Landing gear strut/wheel compression
Nose wheel steering	Main wheel brakes

Table 1. Classification of identification problems

$y = k \cdot y_\infty \cdot h^s$				
	y	y_∞	k	s
$C_{L_{(GE)}}$	$C_{L_{0h}}$	0.827	0.599	-1.45
	$C_{L_{\alpha h}}$	4.87	0.506	-1.75

	$y = k \cdot h^s$		
		k	s
$C_{\ell_{(GE)}}$		-0.078	-1.09

Table 2. Identification of k and s in (13) and (14) for $\delta_f = 40°$

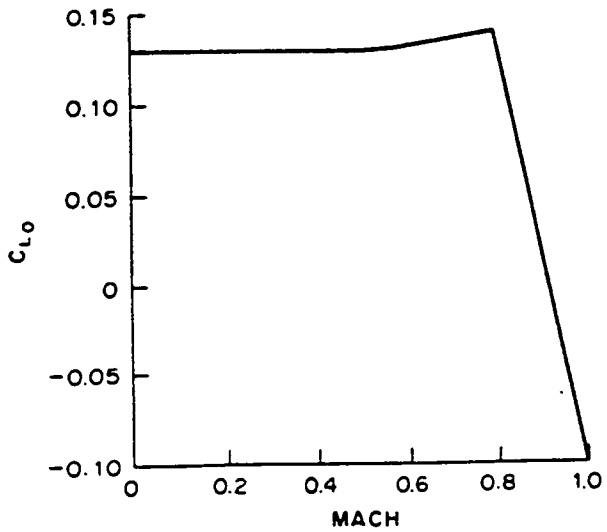

Fig. 1: C_{L_0} as a function of Mach

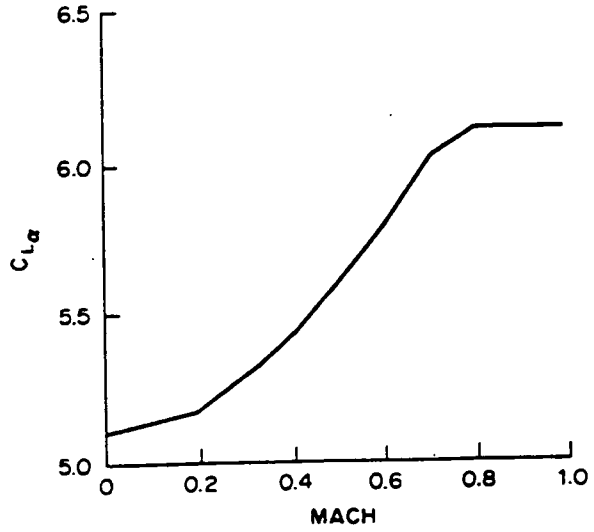

Fig. 2: C_{L_α} as a function of M (clean)

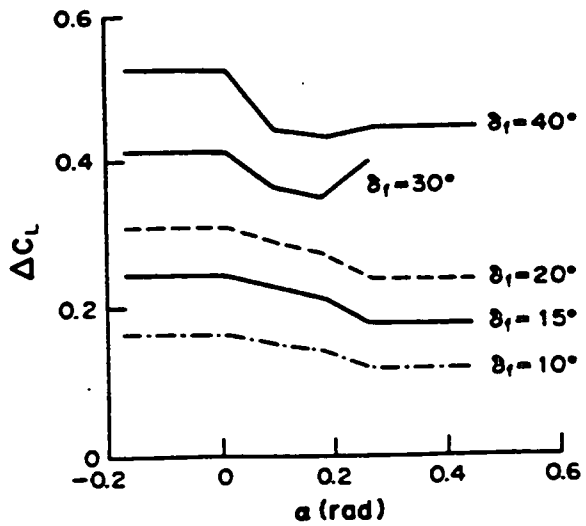

Fig. 3: ΔC_L - α curves for various δ_f

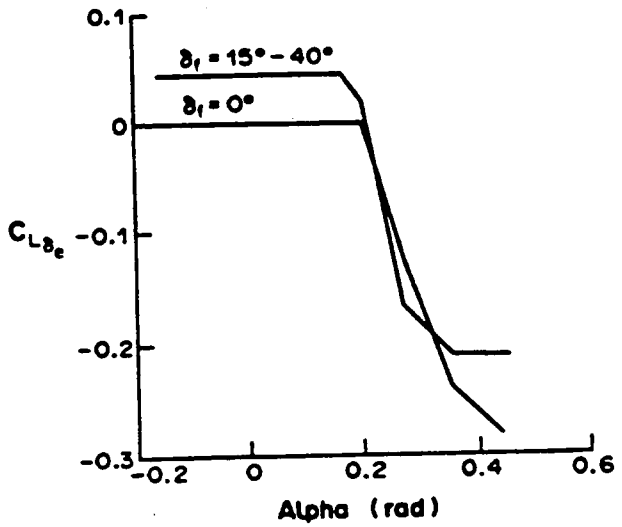

Fig. 4: $C_{L_{\delta_e}}$ as a function of α and δ_f

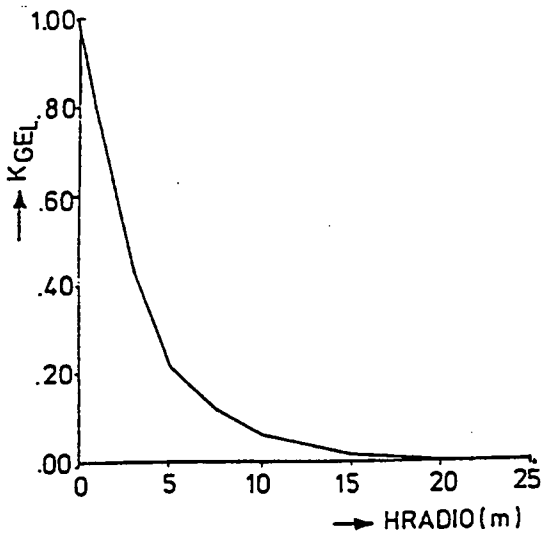

Fig. 5: K_{GE_L} as a function of radio altitude (HRADIO)

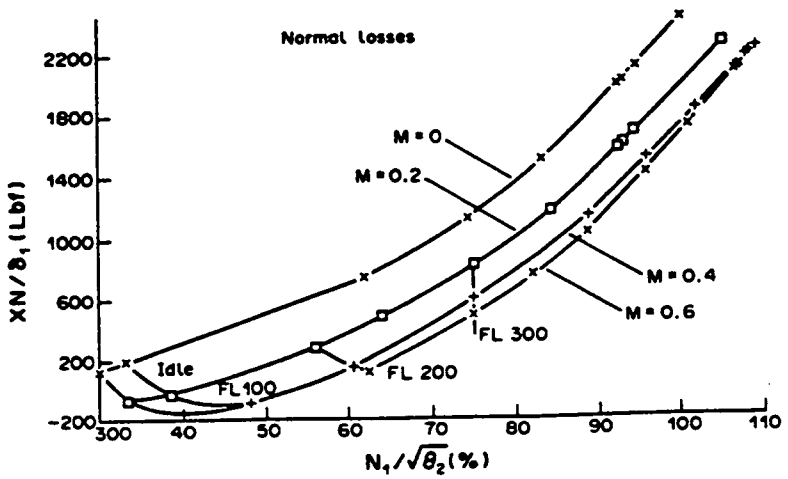

Fig. 6: Net thrust vs fan speed as a function Mach and Flight Level

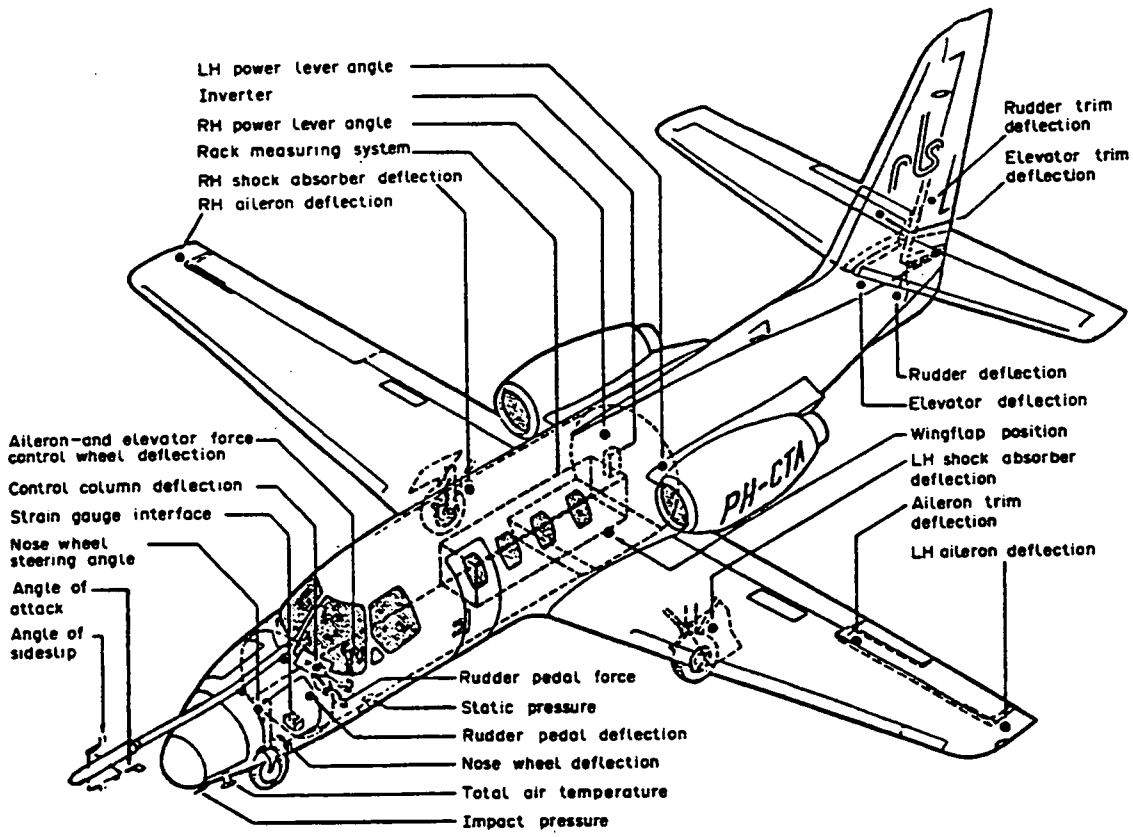

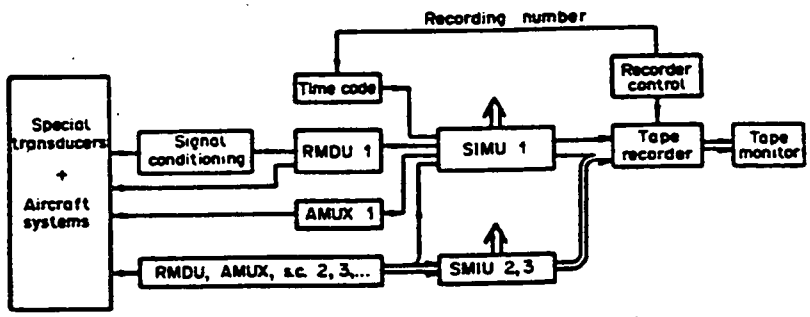

Basic elements of airborne measuring system

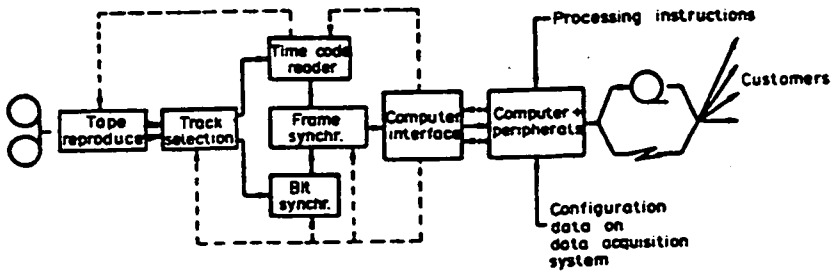

First stage of post flight data processing

Fig. 7: Transducer lay out, airborne measuring system and post flight data processing.

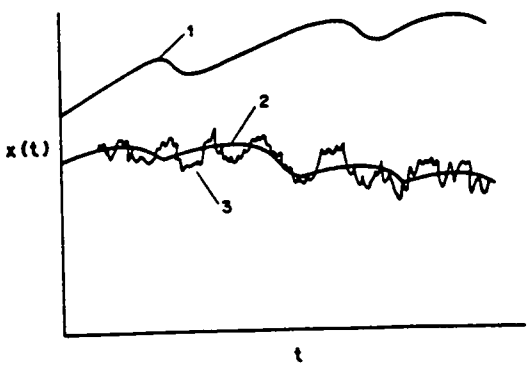

Fig. 8: Principle of model-adjustment

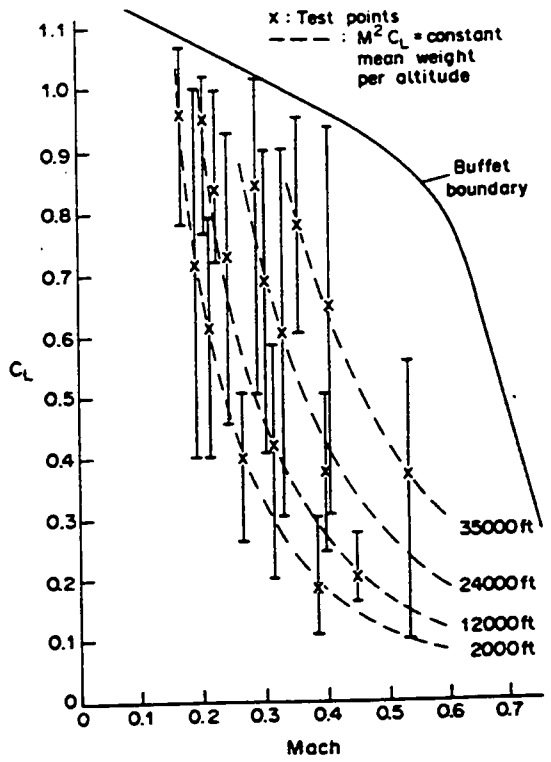

Fig. 9: C_L excursions due to δ_e doublets

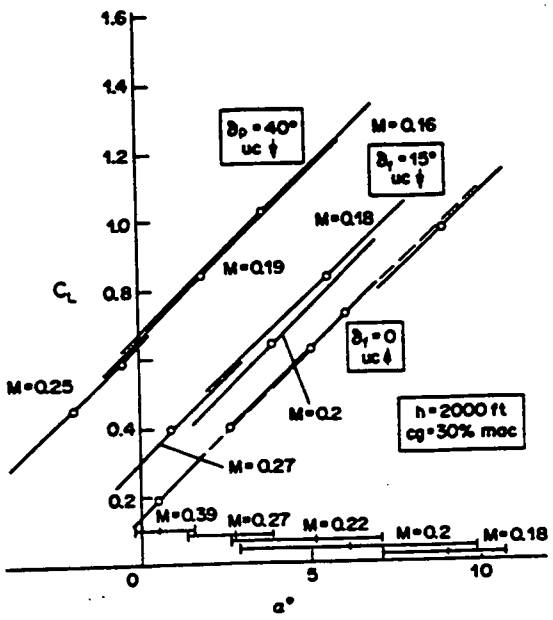

Fig. 10: C_L - α curves for various aircraft config. and Mach

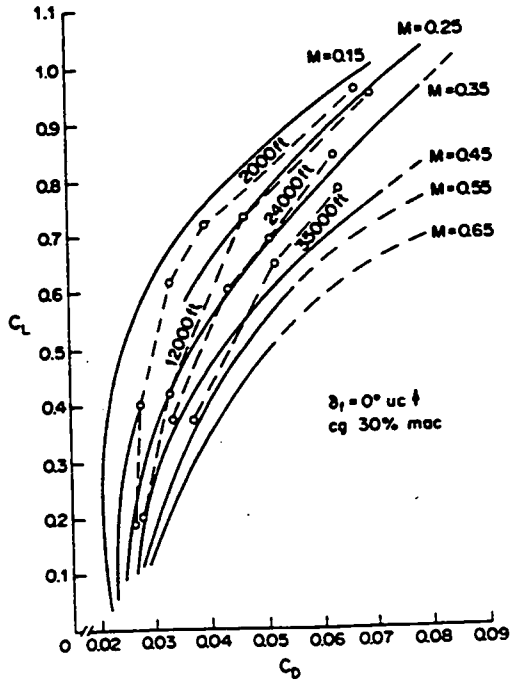

Fig. 11: C_L/C_D curves for various Mach numbers

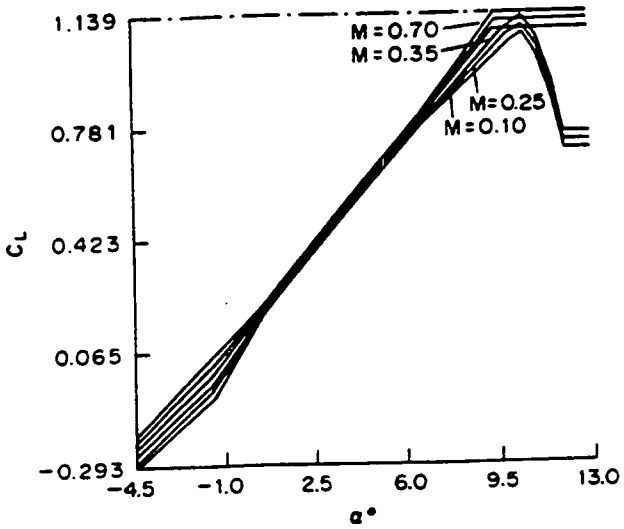

Fig. 12: C_L - α curves for increasing M

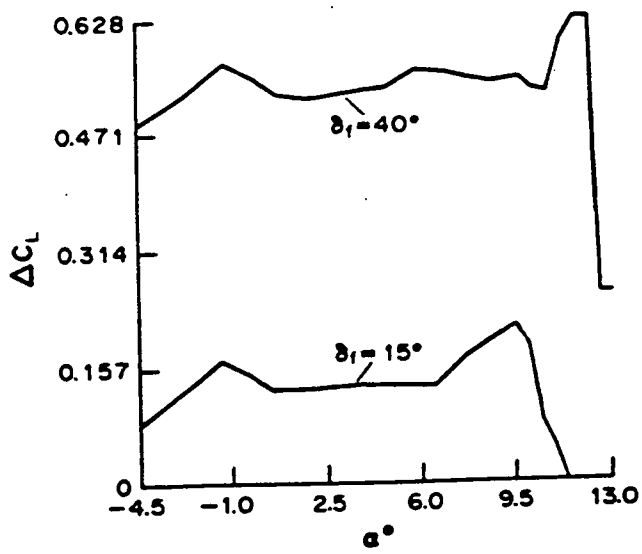

Fig. 13: ΔC_L - α curves for δ_f= 15/40°

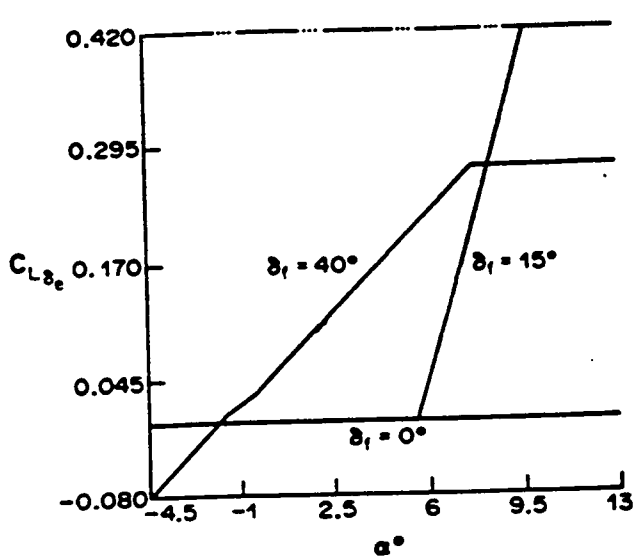

Fig. 14: $C_{L_{\delta_e}}$ - α curves for various δ_f

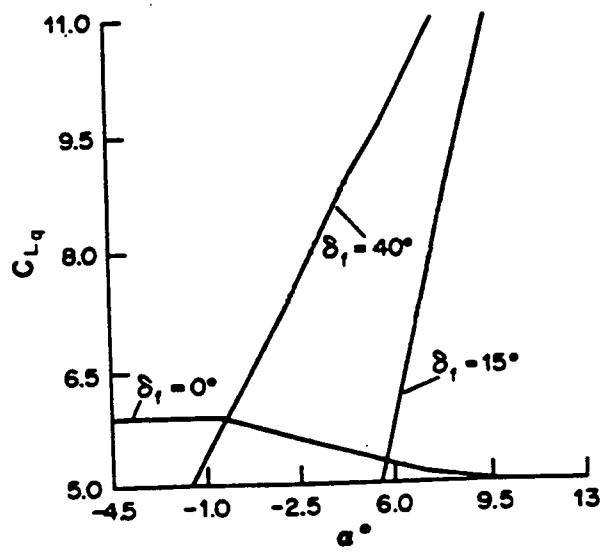

Fig. 15: C_{L_q} - α curves for var. δ_f

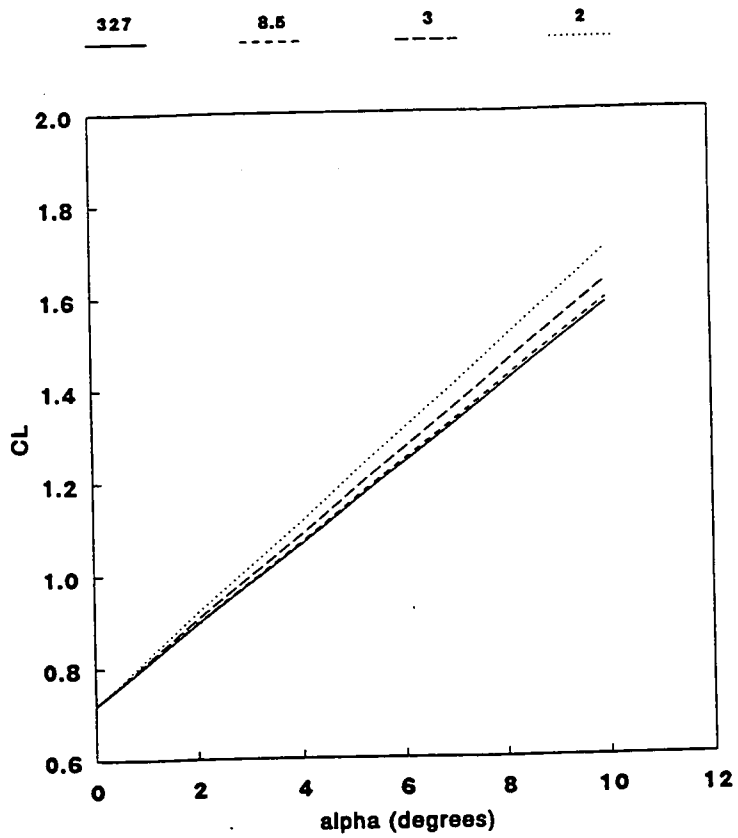

Fig. 16: C_L as a function of α for h = 327, 8.5, 3 and 2m for δ_f= 40°

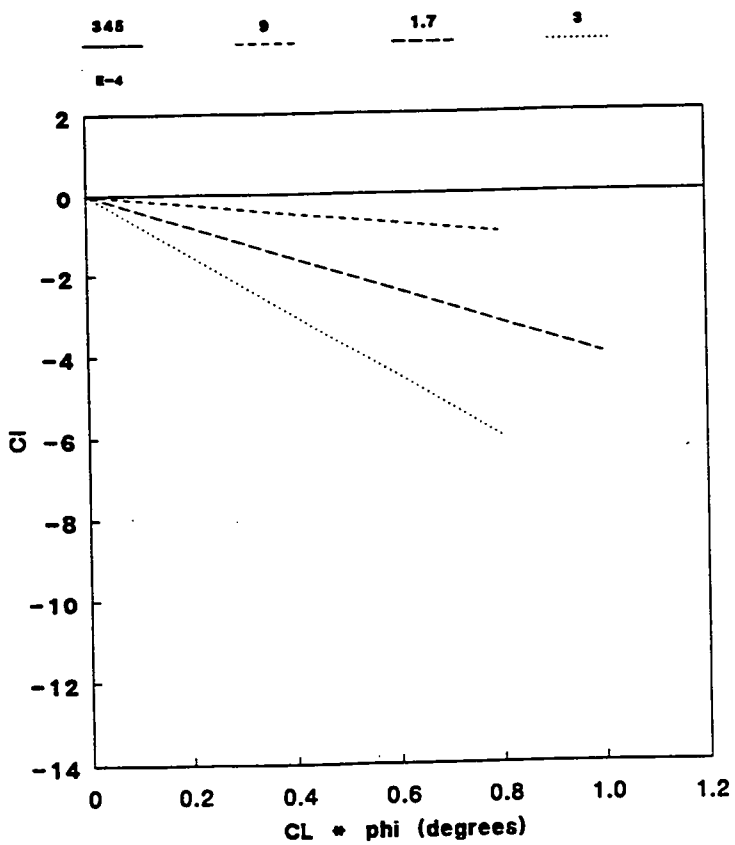

Fig. 17: C_ℓ as a function of $C_L.\phi$ for h = 345, 9, 3 and 1.7m for δ_f= 40°

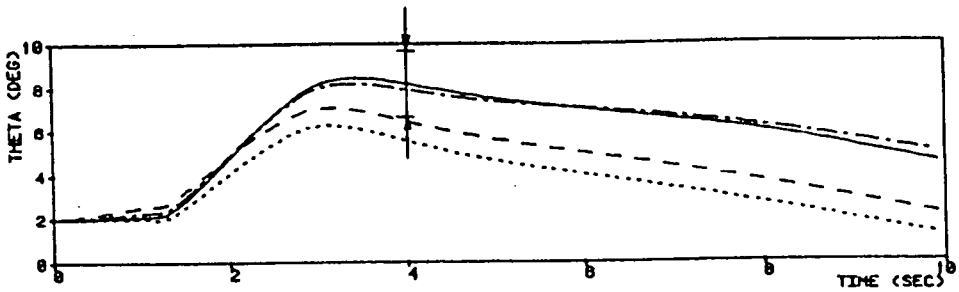

Fig. 18: Short period motion (full flaps, gear down)

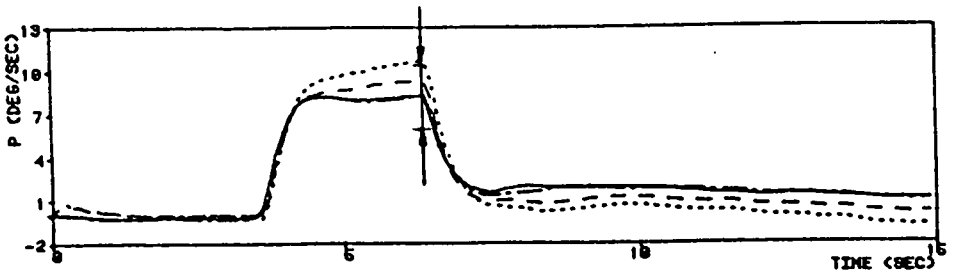

Fig. 19: Roll rate response (clean)

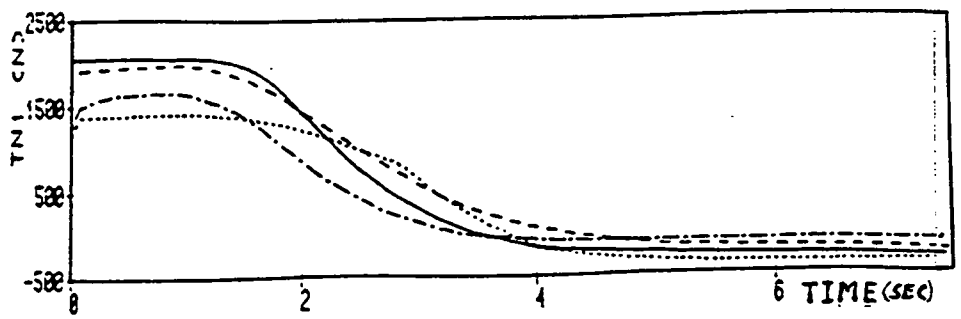

Fig. 20: Power change dynamics (Net Thrust)

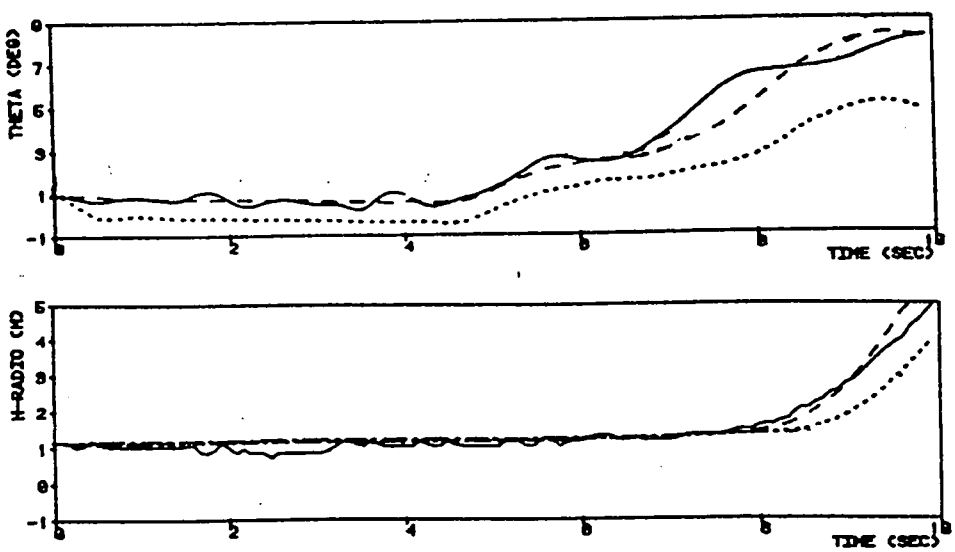

Fig. 21: Normal take-off

_____ measured act response
..... DATCOM based model
------ corrected DATCOM based
_._._. 'final' model